Imaging Epileptogenic Tubers in Children with Tuberous Sclerosis Complex Using α-[^{11}C]Methyl-L-Tryptophan Positron Emission Tomography

Diane C. Chugani, PhD,*† Harry T. Chugani, MD,*†‡ Otto Muzik, PhD,† Jagdish R. Shah, MD,‡ Aashit K. Shah, MD,‡ Alexa Canady, MD,§ Thomas J. Mangner, PhD,† and Pulak K. Chakraborty, PhD†

Several reports have indicated that cortical resection is effective in alleviating intractable epilepsy in children with tuberous sclerosis complex (TSC). Because of the multitude of cortical lesions, however, identifying the epileptogenic tuber(s) is difficult and often requires invasive intracranial electroencephalographic (EEG) monitoring. As increased concentrations of serotonin and serotonin-immunoreactive processes have been reported in resected human epileptic cortex, we used α-[^{11}C]methyl-L-tryptophan ([^{11}C]AMT) positron emission tomography (PET) to test the hypothesis that serotonin synthesis is increased interictally in epileptogenic tubers in patients with TSC. Nine children with TSC and epilepsy, aged 1 to 9 years (mean, 4 years 1 month), were studied. All children underwent scalp video-EEG monitoring, PET scans of glucose metabolism and serotonin synthesis, and EEG monitoring during both PET studies. [^{11}C]AMT scans were coregistered with magnetic resonance imaging and with glucose metabolism scans. Whereas glucose metabolism PET showed multifocal cortical hypometabolism corresponding to the locations of tubers in all 9 children, [^{11}C]AMT uptake was increased in one tuber (n = 3), two tubers (n = 3), three tubers (n = 1), and four tubers (n = 1) in 8 of the 9 children. All other tubers showed decreased [^{11}C]AMT uptake. Ictal EEG data available in 8 children showed seizure onset corresponding to foci of increased [^{11}C]AMT uptake in 4 children (including 2 with intracranial EEG recordings). In 2 children, ictal EEG was nonlocalizing, and in 1 child there was discordance between the region of increased [^{11}C]AMT uptake and the region of ictal onset on EEG. The only child whose [^{11}C]AMT scan showed no regions of increased uptake had a left frontal seizure focus on EEG; however, at the time of his [^{11}C]AMT PET scan, his seizures had come under control. [^{11}C]AMT PET may be a powerful tool in differentiating between epileptogenic and nonepileptogenic tubers in patients with TSC.

Chugani DC, Chugani HT, Muzik O, Shah JR, Shah AK, Canady A, Mangner TJ, Chakraborty PK. Imaging epileptogenic tubers in children with tuberous sclerosis complex using α-[^{11}C]methyl-L-tryptophan positron emission tomography. Ann Neurol 1998;44:858–866

Tuberous sclerosis complex (TSC) is an autosomal dominant inherited disorder with a high spontaneous mutation rate, now known to result from mutations in at least two different genes, TSC1[1,2] and TSC2.[3] These genetic mutations result in tumorous growths in multiple organs, including the brain, skin, heart, and kidney.[4,5] More than 80% of children with TSC have epilepsy due to brain cortical lesions, and for many of these children, the seizures cannot be adequately controlled by medication.[4,6] Although surgical resection of the epileptic focus (consisting of tuber and surrounding epileptogenic tissue) is now being performed to alleviate the intractable epilepsy in children with TSC,[7–10] currently available noninvasive methods do not adequately identify the epileptogenic tuber(s) amid the multiple cortical lesions typical in these patients. As a result, the preoperative evaluation usually includes chronic intracranial electrographic monitoring, which is both invasive and expensive. Clearly, a neuroimaging method that is capable of differentiating between epileptogenic and nonepileptogenic lesions interictally would represent an important advance in the surgical management of children with TSC.[11]

Because increased serotonin (5HT) content[12,13] and immunoreactivity[14] has been reported in human epileptic tissue removed for seizure control, we applied positron emission tomography (PET) with the new tracer α-[^{11}C]methyl-L-tryptophan ([^{11}C]AMT) in

From the Departments of *Pediatrics, †Radiology, ‡Neurology, and §Neurosurgery, Children's Hospital of Michigan and Detroit Medical Center, Wayne State University School of Medicine, Detroit, MI.

Received Feb 17, 1998, and in revised form May 7. Accepted for publication May 8, 1998.

Address correspondence to Dr D. Chugani, PET Center, Children's Hospital of Michigan, 3901 Beaubien Blvd, Detroit, MI 48201.

children with TSC and epilepsy. This method is designed to measure 5HT synthesis in vivo,[15–18] as the intravenously injected [^{11}C]AMT is converted in the brain to α-[^{11}C]methyl-5HT ([^{11}C]AM-5HT), which is not a substrate for the enzyme monoamine oxidase[19] and, therefore, accumulates in serotonergic terminals.

Patients and Methods

Patients

Nine children with TSC and epilepsy were studied. All met the established diagnostic criteria for TSC.[5] There were 5 males and 4 females, aged 1 year 1 month to 9 years 2 months, with a mean age of 4 years 1 month (Table 1). Studies were performed in compliance with regulations of Wayne State University Human Investigation and Radiation Drug Research Committees, and informed consent of parent or guardian was obtained before all [^{11}C]AMT PET scans. Continuous video-electroencephalographic (video-EEG) monitoring was performed to determine the location(s) of seizure onset as a component of the clinical evaluation to determine eligibility for cortical resection. The International 10–20 system for electrode placements was used, and recordings were made on a Biomedical Monitoring Systems (Campbell, CA) 64-channel tape system. Also included in the clinical evaluation were computed tomography, magnetic resonance imaging (MRI), and PET scanning of brain glucose metabolism, using the tracer 2-deoxy-2-[^{18}F]fluoro-D-glucose ([^{18}F]FDG).

[^{11}C]AMT Synthesis and Dosimetry

The [^{11}C]AMT was produced by using a synthesis module designed and built in-house, capable of manipulating the necessary chemistry remotely, using radioactive precursor inside the hot cell.[20,21] Human organ activity and residence time were estimated as previously described.[18] Final values of radiation dose estimates were calculated by using the residence time estimates and the MIRDOSE programs (IBM PC, version 3.0, November 1994) for children of different ages.[22] The dose of [^{11}C]AMT for PET studies in children was 0.1 mCi/kg.

PET Scanning Protocols

The [^{18}F]FDG and [^{11}C]AMT PET scans were performed on different days. The procedure for [^{18}F]FDG PET scanning has been described previously.[23] For the [^{11}C]AMT PET scan, subjects were fasted for 6 hours to obtain stable plasma tryptophan and large neutral amino acid levels during the course of the study. Two venous lines were established, one for tracer injection and one for collection of timed blood samples (0.5 ml/sample, collected at 0, 20, 30, 40, 50, and 60 minutes after [^{11}C]AMT injection); plasma tryptophan concentration was measured in these samples by high-pressure liquid chromatography as previously described.[24,25] Fiduciary markers containing 0.25 μCi [^{11}C]AMT/mCi injected were placed on the scalp to allow for correction of motion, if necessary. Heart rate, blood pressure, and pulse oximetry were measured periodically during the study, and the scalp EEG was monitored continuously. The children were sedated intravenously with either nembutal (5 mg/kg intravenously) or midazolam (0.2–0.4 mg/kg intravenously). Prior studies performed in our laboratory on 5 adult volunteers each scanned twice (once without and once with sedation by using midazolam) have found differences of less than 10% in 5HT synthesis between the two testing conditions (in preparation); these differences are within the accepted test/retest range for PET tracers.[26]

The [^{11}C]AMT (0.1 mCi/kg) was injected intravenously as a slow bolus over 2 minutes. Twenty-five minutes after tracer injection, a dynamic emission scan of the brain (7 × 5 minutes) was acquired in three-dimensional (3D) mode. PET studies were performed by using the CTI/Siemens EXACT/HR whole-body positron tomograph (Knoxville, TN). Measured attenuation and decay correction was applied to all images.

PET Data Processing and Data Analysis

The standardized uptake value (SUV) method for semiquantitative analysis of tracer accumulation was used.[27,28] The SUV represents tissue activity concentration normalized to the injected activity per kilogram of body weight. PET images from time frames 2 to 5 (best image quality) were summed and calibrated to microcuries per cubic centimeter (μCi/cc), representing the retention of [^{11}C]AMT from 30 to 50 minutes after tracer injection. As all subjects received a standardized dose based on their weight (0.1 mCi/kg), calibrated images directly depict the SUV value.[18] [^{11}C]AMT PET scans were coregistered with MRI and [^{18}F]FDG PET scans by using a multipurpose 3D registration technique (MPItool) developed at the Max-Planck-Institute.[29,30] Foci of increased and decreased [^{11}C]AMT uptake were matched with the locations of tubers identified on MRI and [^{18}F]FDG PET scans. Regions of interest were drawn manually around tubers with increased and decreased [^{11}C]AMT uptake and around the surrounding cortex. The average SUV for regions of interest was determined as a weighted average over all planes showing the region. Values for tubers with increased [^{11}C]AMT uptake were compared with regions of surrounding cortex and with tubers with decreased [^{11}C]AMT uptake by using a matched-pairs t test (two-tailed, with Bonferroni correction).

To facilitate the anatomical localization of increased [^{11}C]AMT uptake in Patient 1 in relation to the location of intracranial electrodes on the brain surface, coregistered [^{11}C]AMT PET and MRI volumes were surface rendered by using the Phong illumination model[31] provided by the MEDx software (Senson Systems, Sterling, VA). In brief, given a 3D volume and a surface constant value, the algorithm determines the vertices of all surface polygons and surface normals.[32] These data were then used with the Phong shading algorithm[31] to create a shaded surface of the brain cortex. Both PET and MRI image volumes were 3D-surface rendered, using identical viewing parameters, and the area of increased [^{11}C]AMT uptake was localized on the PET surface, using a maximum intensity projection. On the MRI scan, the position of the grid electrode array on the cortical surface could be recognized due to the small distortions of the magnetic field in the vicinity of the metal electrodes. Finally, the outline of the PET abnormality was transferred to

Table 1. Selected Patient Data

Patient No./ Sex/Age at AMT-PET	Clinical Information	AMT-PET (Medications During PET)	Interictal EEG	Ictal EEG	Epilepsy Surgery
1/female/ 8 yr	At 1 wk, clonic seizures; at 5 mo, infantile spasms; tonic–clonic seizures began at 5 yr; also complex partial seizures; both seizure types intractable (12–14 tonic–clonic seizures/ day) Nonambulatory, nonverbal, severe developmental delay, and severe L hemiparesis	Increased uptake in single large R posterior frontal, parietal, superior temporal tuber; all other tubers showed decreased uptake (lamotrigine and vigabatrin)	Multifocal independent epileptiform activity, especially R parietal, central, and temporal	Onset R parietal–temporal	At 8 yr 2 mo, surgical resection of tuber and surrounding cortical rim showing increased AMT uptake; subdural electrodes placed; not a single seizure since surgery (4 mo), more alert and interactive, no change in L hemiparesis
2/female/2 yr 2 mo	Onset of infantile spasms at 4.5 mo; now has complex partial seizures and tonic seizures Developing normally, with L peripheral visual field deficit	Increased uptake in R frontal and R occipital tubers; decreased uptake in all other tubers (phenobarbital, carbamazepine, and topiramate)	Active R occipital spiking	R occipital onset of seizures; however, clinical onset typically preceded electrographic onset by 20 sec	Being evaluated for epilepsy surgery
3/female/2 yr 10 mo	At 6 wk, complex partial seizures with eyes to L, and vocalizations; at 5 mo, myoclonic jerks; at 7 mo, infantile spasms. At present, tonic–clonic seizures (L > R involvement), 20–40/day, also complex partial seizures, mild developmental delay, and subtle L hemiparesis	Increased uptake in R superior posterior frontal tuber adjacent to previous resection, and in another tuber in R inferior frontal cortex; all other tubers showed decreased uptake (carbamazpine)	Multifocal independent epileptiform activity with R central temporal predominance	R frontal onset of seizures	At 2 yr at another institution, partial resection of R frontal tuber following subdural electrodes, shoulder area of motor cortex involved, but not resected; seizures continued; at 3 yr 3 mo, at another (different) institution, further resection of tuber with increased AMT uptake; resection limited because of proximity to motor cortex; tonic–clonic seizures subsided, complex partial seizures continued
4/male/2 yr 3 mo	At 5 wk, onset of seizures with L arm flexion; now stares and verbalizes during seizures; mild L hemiparesis and mild cognitive delay	Increased uptake in R superior frontal tuber and R inferior frontal tuber; all other tubers showed decreased uptake (vigabatrin)	Multifocal independent epileptiform activity especially L frontal, L central, and R temporal	Right frontal onset at F_4 and FP_2	Considering epilepsy surgery
5/female/9 yr 2 mo	At 4 mo, infantile spasms; now tonic–clonic seizures followed by clusters of head drops; also has complex partial seizures	Increased uptake in R posterior temporal tuber; all other tubers showed decreased uptake (valproate)	Generalized polyphasic spike and wave activity and independently from L frontal–temporal and R temporal	Right hemisphere onset, could not be further localized	Considering epilepsy surgery
6/male/3 yr	Onset of complex partial seizures at 1.5 yr, now has frequent secondary generalization; behavioral disorder and autistic; mother and her 2 sisters have TSC	Increased uptake in L medial parietal tuber; all other tubers showed decreased uptake (valproate)	Multifocal epileptiform discharges, most prominent L parietal and L temporal	Not done	Not actively being pursued
7/female/ 7 yr	Onset of clonic seizures at 1 day of age; at 4 mo, infantile spasms; now tonic seizures, sometimes preceded by a head drop; no speech, nonambulatory, and L handed	Increased uptake in R posterior frontal tuber, R inferior frontal tuber, and R posterior temporal tuber; all other tubers show decreased uptake (vigabatrin, clonazepam, phenobarbital, and ketogenic diet)	Multifocal independent epileptiform activity	L frontal onset of seizures	Not being considered
8/male/3 mo (1st scan) and 1 yr 1 mo (2nd scan)	At 2.5 mo, complex partial seizures; at 3 mo, infantile spasms; seizures now reasonably well controlled with occasional breakthrough of spasms; mild right-hand weakness	1st scan, increased uptake of tuber in R temporal pole (carbamazepine and vigabatrin); 2nd scan, increased uptake of tubers in R temporal pole, R inferior frontal cortex, and 2 in R parietal cortex (carbamazepine, vigabatrin, and nitrazepam)	Multifocal independent epileptiform activity, especially F_8, T_4, and T_6	Onset could not be localized or lateralized	Not being considered
9/male/1 yr 7 mo	Age 4 mo, onset of infantile spasms, responded to vigabatrin; seizure free until 1 yr 4 mo when developed complex partial seizures, now controlled; slight speech delay, otherwise developing normally; normal exam	All tubers show decreased uptake (vigabatrin and carbamazepine); this child's seizures had come under control at the time of the scan	Independent frontal sharp waves; generalized spike and slow wave bursts during sleep with L predominance	Onset L frontal (F_3)	Not being considered

AMT-PET = positron emission tomography (PET) with tracer α-[^{11}C] methyl-L-tryptophan (AMT); EEG = electroencephalography; L = left; R = right; TSC = tuberous sclerosis complex.

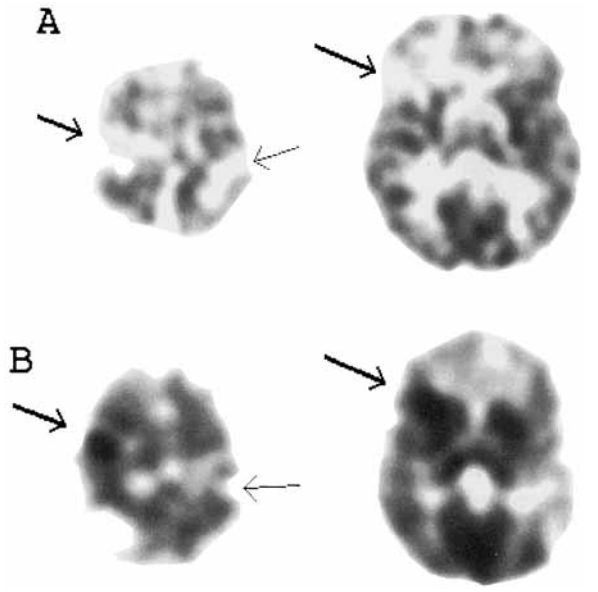

Fig 1. Positron emission tomographic (PET) scans in a 2-year-old boy (Patient 4) with tuberous sclerosis complex and intractable epilepsy. (A) The 2-deoxy-2-[^{18}F]fluoro-D-glucose PET scan shows multiple regions of cortical hypometabolism corresponding to the location of tubers (arrows). *(B) α-[^{11}C]methyl-L-tryptophan ([^{11}C]AMT) standardized uptake value (SUV) images display multiple regions of decreased tracer uptake in the location of tubers compared with nonlesional cortex* (thin arrows). *Two regions in right frontal cortex display a large increase in [^{11}C]AMT uptake with a nodular distribution* (bold arrows). *Video-electroencephalographic monitoring of seizures revealed the right frontal lobe to be the region of ictal onset. The left side of the image is the right side of the brain.*

the MRI surface, to determine the location of the PET abnormality relative to the location of electrodes overlying regions of ictal onset.

Results

The findings on [^{11}C]AMT PET scans, as well as interictal and ictal EEG, are summarized in Table 1. [^{18}F]FDG PET images revealed multiple foci of decreased glucose metabolism in cortical regions corresponding to locations of tubers (Figs 1–3); these results are consistent with previous reports.[11,33] Examination of the [^{11}C]AMT SUV images also showed multiple foci of reduced tracer uptake compared with surrounding cortex; however, there were also focal regions of increased tracer uptake in the cortex. Ratios of SUVs for tubers with increased [^{11}C]AMT uptake to surrounding cortex and tubers with low [^{11}C]AMT are shown in Table 2. Three children showed one region of increased uptake (see Fig 3), another 3 children showed two regions (see Figs 1 and 2), and 1 subject each showed three and four regions of increased [^{11}C]AMT uptake (see Tables 1 and 2). The magnitude of focal increase relative to adjacent cortex ranged from 5 to 111% (25 ± 25%, mean ± SD; $p = 0.01$). SUV values in tubers with increased [^{11}C]AMT uptake were 20 to 188% (61 ± 44%, mean ± SD; $p = 0.003$) higher than in tubers with low uptake from the same subject.

Eight of the 9 children have undergone scalp video-EEG monitoring to localize seizure onset for potential cortical resection. One of these (Patient 9) had a left frontal seizure focus, but his seizures were controlled at the time of [^{11}C]AMT PET, which did not show any regions of increased [^{11}C]AMT uptake. Of the remaining 7 children who had undergone video-EEG monitoring, 4 showed excellent correspondence between seizure foci and regions of increased [^{11}C]AMT uptake (Patients 1 through 4), but there was poor correspondence in 1 child (Patient 7). In 2 children (Patients 5 and 8), ictal EEG recordings failed to localize the seizure foci; however, in 1 of these (Patient 5), the ictal EEG lateralized seizure onset to the same hemisphere as the focus of increased [^{11}C]AMT uptake. Patient 8 was studied twice with [^{11}C]AMT PET; at 3 months,

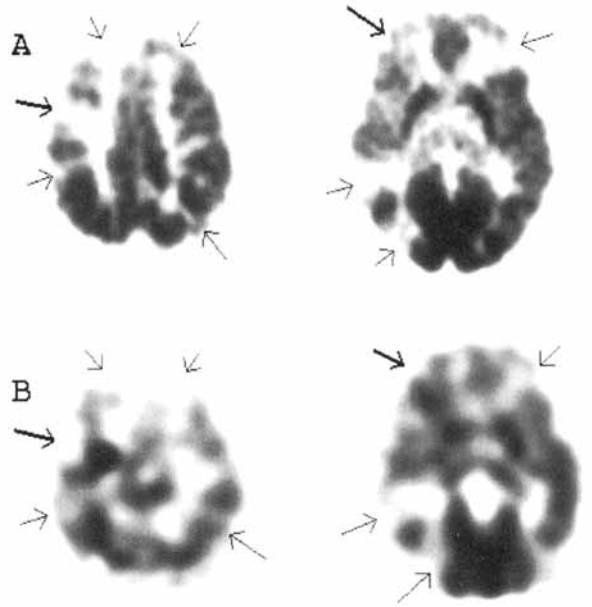

Fig 2. Positron emission tomographic (PET) scans in a 2-year-old girl (Patient 3) with tuberous sclerosis complex and intractable epilepsy. (A) The 2-deoxy-2-[^{18}F]fluoro-D-glucose PET scan shows multiple regions of cortical hypometabolism corresponding to the location of tubers (arrows). *(B) The α-[^{11}C]methyl-L-tryptophan ([^{11}C]AMT) standardized uptake value PET scans show a nodular region of increased [^{11}C]AMT uptake in the right frontal/central region* (bold arrow). *In addition, there is a region of increased [^{11}C]AMT uptake of smaller magnitude surrounding a tuber in the right inferior frontal lobe* (bold arrow). Thin arrows *denote tubers with decreased [^{11}C]AMT uptake. The left side of the image is the right side of the brain.*

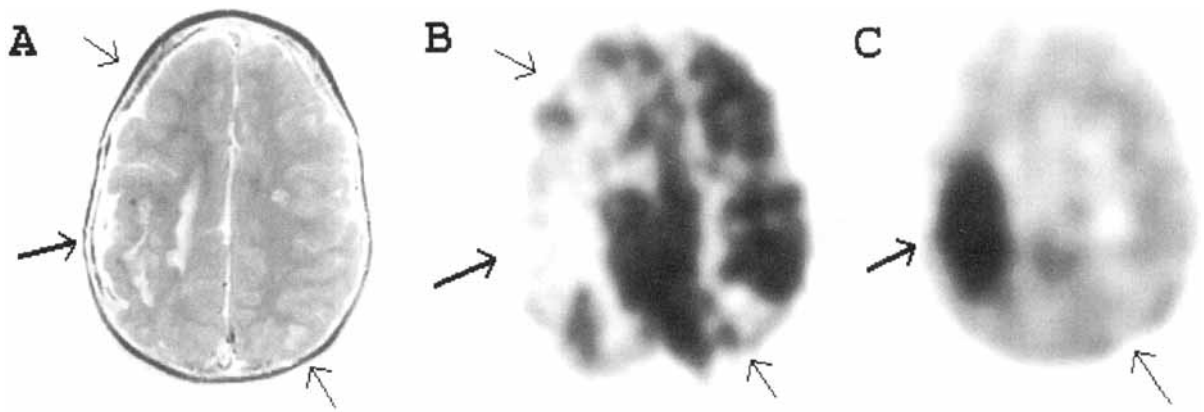

Fig 3. Magnetic resonance imaging (MRI) and positron emission tomographic (PET) scans in an 8-year-old girl (Patient 1) with tuberous sclerosis complex and intractable epilepsy. (A) MRI scan showing large tuber in the right central/parietal region (bold arrow) *as well as other smaller lesions* (thin arrows). *(B) The glucose metabolism PET scan shows cortical hypometabolism in the same regions as the lesions seen on MRI* (arrows). *(C) α-[^{11}C]methyl-L-tryptophan ([^{11}C]AMT) standardized uptake value images display decreased tracer uptake in the location of small tubers compared with adjacent nonlesional cortex* (thin arrow). *The large right central tuber* (bold arrow) *shows a 110% increase in [^{11}C]AMT uptake. The left side of the image is the right side of the brain.*

Table 2. Ratios of SUVs for Tubers with Increased [^{11}C]AMT Uptake to Adjacent Cortex and to Tubers with Low [^{11}C]AMT Uptake

Patient No.	Tuber Location	Tuber/ Cortex	Tuber/ Other Tubers
1	R frontal/temporal/parietal	2.108	2.882
2	R frontal	1.298	1.639
	R occipital	1.211	1.812
3	R superior frontal	1.327	1.829
	R inferior frontal	1.091	1.578
4	R superior frontal	1.393	2.048
	R inferior frontal	1.438	2.084
5	R temporal	1.111	1.270
6	L parietal	1.110	1.197
7	R posterior frontal	1.111	1.214
	R inferior frontal	1.045	1.276
	R posterior temporal	1.144	1.325
8	R temporal	1.104	1.374
	R inferior frontal	1.214	1.453
	R parietal	1.170	1.411
	R parietal	1.126	1.489
9	None		
Mean		1.250	1.618
Standard deviation		0.255	0.439

SUV = standardized uptake value; [^{11}C]AMT = α-[^{11}C]methyl-L-tryptophan.

he showed a single focus of increased [^{11}C]AMT uptake, but at 1 year 1 month he showed three additional foci of increased [^{11}C]AMT uptake in the vicinity of the first focus (see Table 1).

To date, 2 of the children (Patients 1 and 3) have undergone surgical resection of the [^{11}C]AMT focus. Their results are summarized in Table 1. In Patient 1, intracranial subdural grid electrode arrays were placed on posterior frontal, parietal, and temporal cortex for more precise localization of ictal onset before resective surgery. A volumetric MRI scan acquired with subdural electrodes in place was coregistered with the [^{11}C]AMT PET scan, and both MRI and PET scans underwent a maximum intensity projection in 3D. The region of increased [^{11}C]AMT uptake was delineated and superimposed on the MRI showing the position of the subdural electrodes (Fig 4). During the intracranial monitoring period, the patient had 10 of her typical seizures. Eight of these seizures originated at electrodes at the posterior border of the [^{11}C]AMT PET abnormality (Fig 5A), but the remaining two could not be localized. The eight seizures showed rapid spread to the anterior and inferior borders of the [^{11}C]AMT PET abnormality (see Fig 5B).

Discussion

Methodological Issues

In the present study, the SUV method was applied, because these images are of higher quality than parametric images with [^{11}C]AMT,[17,18] facilitating the localization of focal abnormalities. The SUV method[27,28] is a semiquantitative method, widely used in assessing metabolic activity in tumors by using [^{18}F]FDG PET,[34,35] because absolute values of the glucose metabolic rate are difficult to obtain due to several unknown variables in tumors, including the lumped constant, a factor explaining differences between the kinetics of tracer and natural substrate. Likewise, the lumped constant for [^{11}C]AMT in humans is unknown, and appears to be species specific.[36,37] The SUV in various regions of brain is equal to the sum of

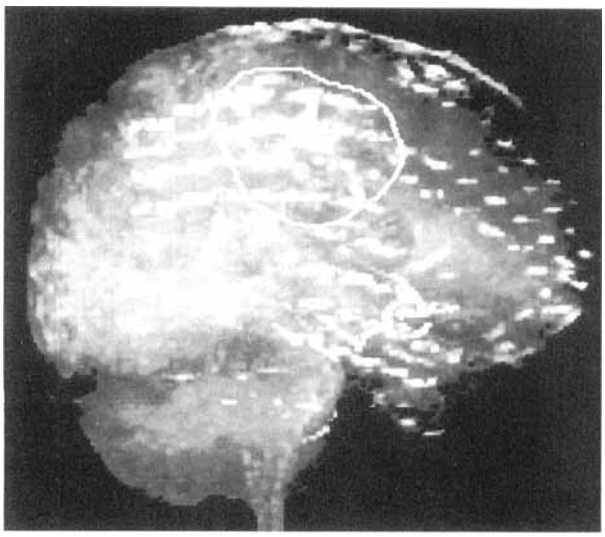

Fig 4. Magnetic resonance imaging three-dimensional rendered image (Patient 1), using a maximum intensity projection showing location of subdural grid electrode placement and delineation of region of increased α-[^{11}C]tmethyl-L-ryptophan ([^{11}C]AMT) uptake. The position of the grid electrode array on top of the exposed cortical surface can be recognized due to the small distortions of the magnetic field in the vicinity of the metal electrodes. The circular line delineates the region of increased [^{11}C]AMT uptake in the frontoparietal region.

the precursor [^{11}C]AMT and the metabolic product [^{11}C]AM-5HT synthesized in these regions. We have previously reported an excellent correlation between regional values of the unidirectional uptake rate constant K and regional SUV.[18] In another neurological disorder of childhood (ie, autism), we have established that the SUV analytic approach is sensitive in depicting focal abnormalities.[38]

Epilepsy and Neuroimaging in TSC

Intracranial lesions in TSC include cortical tubers,[39–41] subependymal nodules, subependymal giant cell astrocytoma,[42] and microscopic abnormalities such as microdysgenesis, heterotopic gray matter, and lamination defects.[41,43] More than 80% of patients with TSC have seizures, and when these are uncontrolled, the prognosis is poor for normal cognitive function.[4,44] Recent attempts at surgical removal of the epileptogenic tuber(s) have met with some success,[7–10] but the preoperative evaluation is generally invasive due to the frequent requirement of intracranial EEG monitoring with subdural electrodes. Scalp EEG localization may identify the lobe in which seizures are generated; however, this lobe may contain multiple tubers, only one of which may be responsible for the seizures. Anatomical neuroimaging with computed tomography and MRI may demonstrate precisely the locations of tubers and calcifications[44–48] but does not differentiate between epileptogenic and nonepileptogenic zones in the brain. Even currently available functional imaging studies are of limited use in patients with TSC. PET scanning with [^{18}F]FDG shows decreased glucose metabolism corresponding to the locations of tubers and calcifications[11,33] but is not capable of distinguishing between epileptogenic and nonepileptogenic lesions, unless a prolonged seizure fortuitously occurs during the tracer uptake period, leading to focally increased glucose metabolism (ictal PET study).[49] Because of the short half-lives of PET isotopes, however, ictal PET studies are not practical. Although ictal studies by using single-photon emission computed tomography (SPECT) have enjoyed more success in this regard, these are particularly difficult to accomplish in children with TSC, whose seizures are typically short lasting and are not ideal for ictal SPECT study. Because of this, and its relatively poor spatial resolution, SPECT has not been applied routinely in the presurgical evaluation of patients with TSC and intractable epilepsy.

The development of a specific PET probe capable of differentiating between epileptogenic and nonepileptogenic tubers is an important advance in the neurological management of patients with TSC and intractable epilepsy. Our laboratory has been attempting to develop such a probe for several years. Our initial efforts with [^{11}C]flumazenil PET to measure benzodiazepine receptor binding in patients with TSC have not been successful in this regard, showing decreased receptor binding in all tubers and calcified regions, with no specificity for epileptogenicity (Chugani and colleagues, unpublished data). The present findings with [^{11}C]AMT PET in patients with TSC and uncontrolled seizures strongly suggest that epileptogenic tubers (characterized by high [^{11}C]AMT uptake) can be differentiated from nonepileptogenic ones (characterized by low [^{11}C]AMT uptake). Coregistration of the [^{11}C]AMT PET images with MRI (see Figs 3 and 4) provides the necessary accurate spatial localization of the cortical lesions with high [^{11}C]AMT uptake, which appear to correspond to EEG localization of seizure onset. Although subependymal lesions were present in all 9 children, none of these lesions could be visualized on the [^{11}C]AMT PET scans, consistent with the notion that subependymal lesions are not epileptogenic.

At present, only 2 of the 9 children studied have undergone surgical resection of the lesion showing increased [^{11}C]AMT uptake (Patient 3 underwent surgery at another institution), and another 3 children are being considered for surgery. Both of the resections performed were guided by corticographic recordings from subdural electrodes, which showed excellent correspondence between seizure onset and [^{11}C]AMT foci (see Table 1, Figs 4 and 5). It is unfortunate that a larger resection could not be performed in Patient 3

Fig 5. Subdural electroencephalographic recording (Patient 1) showing ictal onset at electrodes 58 and 59, which were located at the posterior border of the tuber, with increased α-[^{11}C]methyl-L-tryptophan uptake (A) and spread of seizure to electrodes 8 and 16 around the border of the tuber (B) (referential recording; reference is inactive electrode 1).

because of the proximity of the seizure focus to primary motor cortex.

The findings in Patient 2 are interesting and deserve some comment. Both interictal and ictal EEG in this child suggested a right occipital focus, but clinical onset of each seizure preceded electrographic onset by 20 seconds or more. [^{11}C]AMT uptake was increased, as expected, in a right occipital tuber, but a second tuber in the right frontal cortex also showed increased uptake. The significance of this finding is not clear at present but may suggest that at least some of the seizures may have their onset in the right frontal lobe. A discussion of Patient 7, in whom ictal EEG and [^{11}C]AMT PET appear to be discordant, is warranted. The magnitude of the increased [^{11}C]AMT uptake in right cortical regions of Patient 7 was not as large as measured in most subjects (see Table 2). Therefore, perhaps only tubers with larger increases of [^{11}C]AMT uptake might be reliable in the designation of epileptogenic tubers. It is also possible, however, that the EEG is falsely lateralizing in this case due the presence of a large tuber in the right inferior frontal cortex adjacent to the midline. Finally, the lack of any regions with increased [^{11}C]AMT uptake in Patient 9, whose seizures were medically controlled at the time of the [^{11}C]AMT PET scan, suggests that the biochemical changes in epileptogenic tubers resulting in increased [^{11}C]AMT may be reversible with seizure control.

Role of 5HT in Epilepsy

There are several lines of evidence implicating serotonergic mechanisms as playing a role in epileptogenesis. In the genetically epilepsy-prone rat model of generalized epilepsy, there is a decrease in brain concentration of 5HT,[50] as well as decreased V_{max} for [^{3}H]5HT uptake by synaptosomes and tryptophan hydroxylase ac-

tivity.[51] Pharmacological treatments that facilitate serotonergic neurotransmission inhibit seizures in many animal models of epilepsy, including the genetically epilepsy-prone rat, maximal electroshock model, pentylenetetrazol administration, kindling, and bicuculline microinjections in the area tempestas.[51] Conversely, the lowering of brain 5HT concentrations leads to an increase in seizure susceptibility in animal models of epilepsy[52,53] as well as in humans.[54,55] Finally, in human brain tissue surgically removed for seizure control, levels of 5-HIAA (5-hydroxyindole acetic acid, the breakdown product of 5HT) were found to be higher in actively spiking temporal cortex, compared with normal controls.[12,13] Increased 5HT immunoreactivity has also been reported in human epileptic brain tissue resected for the control of epilepsy.[14]

The data from human epileptic tissue cited above are consistent with the findings reported in the present study, as well as in non-TSC children with epilepsy,[56] which show that increased 5HT synthesis measured with [^{11}C]AMT PET also correctly identifies epileptogenic cortex as indicated by ictal scalp EEG recordings. Our results, although preliminary, are encouraging and suggest that the development of PET probes with increasing specificity for epileptogenic brain regions is feasible and should be a logical next step in the application of neuroimaging to localize epileptogenic brain regions. Clearly, our findings must be confirmed in a larger group of subjects with epilepsy and multifocal lesions.

These studies were funded in part by a grant from the National Tuberous Sclerosis Association.

We are indebted to Dr Donald Kuhn for performing plasma tryptophan measurements and to the staff of the PET Center of Children's Hospital of Michigan for their assistance in performing these studies.

References

1. Fryer AE, Chalmers A, Conner JM, et al. Evidence that the gene for tuberous sclerosis is on chromosome 9. Lancet 1987; 1:659–661
2. van Slegtenhorst M, de Hoogt R, Hermans C, et al. Identification of the tuberous sclerosis gene TSC1 on chromosome 9q34. Science 1997;277:805–808
3. Kandt RS, Haines JL, Smith M, et al. Linkage of an important gene locus for tuberous sclerosis to a chromosome 16 marker for polycystic kidney disease. Nat Genet 1992;2:37–41
4. Gomez MR. Neurologic and psychiatric features. In: Gomez MR, ed. Tuberous sclerosis. New York: Raven Press, 1988: 21–36
5. Roach ES, Smith M, Huttenlocher P, et al. Report of the diagnostic criteria committee of the National Tuberous Sclerosis Association. J Child Neurol 1992;7:221–224
6. Gomez M. Tuberous sclerosis. In: Gomez MR, ed. Neurocutaneous diseases. Boston: Butterworths, 1987:30–52
7. Bye AM, Matheson JM, Tobias VH, Mackensie RA. Selective epilepsy surgery in tuberous sclerosis. Aust Paediatr J 1989;25: 243–245
8. Andermann F, Palmini AL. Neuronal migration disorders, tuberous sclerosis, and Sturge-Weber syndrome. In: Epilepsy surgery. New York: Raven Press, 1992:203–211
9. Duchowny M, Levin B, Jayakar P, et al. Temporal lobectomy in early childhood. Epilepsia 1992;33:298–303
10. Bebin EM, Kelly PJ, Gomez MR. Surgical treatment for epilepsy in cerebral tuberous sclerosis. Epilepsia 1993;34:651–657
11. Rintahaka PJ, Chugani HT. Clinical role of positron emission tomography in children with tuberous sclerosis complex. J Child Neurol 1997;12:42–52
12. Louw D, Sutherland GB, Glavin GB, Girvin J. A study of monoamine metabolism in human epilepsy. Can J Neurol Sci 1989;16:394–397
13. Pintor M, Mefford IN, Hutter I, et al. The levels of biogenic amines, their metabolites and tyrosine hydroxylase in the human epileptic temporal cortex. Synapse 1990;5:152–156
14. Trottier S, Evrard B, Vignal JP, et al. The serotonergic innervation of the cerebral cortex in man and its changes in focal cortical dysplasia. Epilepsy Res 1996;25:79–106
15. Diksic M, Nagahiro S, Sourkes TL, Yamamoto YL. A new method to measure brain serotonin synthesis in vivo. I. Theory and basic data for a biological model. J Cereb Blood Flow Metab 1990;9:1–12
16. Nishizawa S, Benkelfat C, Young SN, et al. Differences between males and females in rates of serotonin synthesis in human brain. Proc Natl Acad Sci USA 1997;94:5308–5313
17. Muzik O, Chugani DC, Chakraborty PK, et al. Analysis of (C-11]alpha-methyl-tryptophan kinetics for the estimation of serotonin synthesis rate in vivo. J Cereb Blood Flow Metab 1997;17:659–669
18. Chugani DC, Muzik O, Chakraborty PK, et al. Human brain serotonin synthesis capacity measured in vivo with α[C-11]-methyl-L-tryptophan. Synapse 1998;28:33–43
19. Missala K, Sourkes TL. Functional cerebral activity of an analogue of serotonin formed in situ. Neurochem Int 1988;12: 209–214
20. Chakraborty PK, Mangner TJ, Chugani DC, et al. A high yield and simplified procedure for the synthesis of α[C-11]methyl-L-tryptophan. J Label Comp Radiopharmacol 1995;37:619–621
21. Chakraborty PK, Mangner TJ, Chugani DC, et al. A high yield and simplified procedure for the synthesis of α[C-11]methyl-L-tryptophan. Nucl Med Biol 1996;23:1005–1008
22. Muzik O, Chugani DC, Shen C, da Silva E. Non-invasive imaging of serotonin synthesis rate using PET and [C-11]alpha-methyl-tryptophan. In: Carson RE, Daube-Witherspoon ME, Hercovitch P, eds. Quantitative functional brain imaging with positron emission tomography. New York: Academic Press, 1997:201–206
23. Chugani HT, Phelps ME, Mazziotta JC. Positron emission tomography study of human brain functional development. Ann Neurol 1987;22:487–497
24. Kuhn DM, Lovenberg W. Assays of serotonin, related metabolites and tryptophan hydroxylase. In: Parvez H, Parvez S, Nagatsu I, Natasu T, eds. Methods in biogenic amine research. Amsterdam: Elsevier, 1983:515–548
25. Wolf WA, Kuhn DM. The uptake and release of tryptophan and serotonin: an HPLC method to study the flux of endogenous 5-hydroxyindoles through synaptosomes. J Neurochem 1986;46:61–67
26. Brooks RA, Di Chiro G, Zukerberg BW, et al. Test-retest studies of cerebral glucose metabolism using fluorine-18 deoxyglucose: validation of method. J Nucl Med 1987;28: 53–59
27. Kenney JM, Marinelli LD, Woodard HQ. Tracer studies with

radioactive phosphorus in malignant neoplastic disease. Radiology 1941;37:683–690
28. Woodard HQ, Gigler RE, Freed B, Russ G. Expression of tissue isotope distribution. J Nucl Med 1975;16:958–959
29. Pietrzyk U, Herholz K, Heiss WD. Three-dimensional alignment of functional and morphological tomograms. J Comput Assist Tomogr 1990;14:51–59
30. Pietrzyk U, Herholz K, Fink G, et al. An interactive technique for three-dimensional image registration: validation for PET, SPECT, MRI and CT brain studies. J Nucl Med 1994;35: 2011–2018
31. Foley J, van Dam A, Feiner S, Hughes J. Computer graphics: principles and practice. Menlo Park, CA: Addison-Wesley, 1990:702
32. Lorenson C, Kline D. "Marching cubes": a high resolution 3D-surface construction algorithm. Comput Graphics 1987;21: 163–169
33. Szelies B, Herholz K, Heiss WD, et al. Hypometabolic cortical lesions in tuberous sclerosis with epilepsy: demonstration by positron emission tomography. J Comput Assist Tomogr 1983; 7:946–953
34. Strauss LG, Conti PS. The applications of PET in clinical oncology. J Nucl Med 1991;32:623–647
35. Gupta NC, Frank AR, Dewan NA, et al. Solitary pulmonary nodules: detection of malignancy with PET with 2-[F-18]-fluoro-2-deoxy-D-glucose. Radiology 1992;184:441–444
36. Vanier M, Tsuiki K, Grdisa M, et al. Determination of the lumped constant for the α-methyltryptophan method of estimating the rate of serotonin synthesis. J Neurochem 1995;64: 624–635
37. Shoaf SE, Schmall B. Pharmacokinetics of α-methyl-L-tryptophan in rhesus monkeys and calculation of the lumped constant for estimating the rate of serotonin synthesis. J Pharmacol Exp Ther 1996;277:219–224
38. Chugani DC, Muzik O, Rothermel R, et al. Altered serotonin synthesis in the dentatothalamocortical pathway in autistic boys. Ann Neurol 1997;42:666–669
39. Ferrer I, Fabregues I, Coll J, et al. Tuberous sclerosis: a Golgi study of cortical tuber. Clin Neuropathol 1984;3:47–51
40. Huttenlocher PR, Heydemann PT. Fine structure of cortical tubers in tuberous sclerosis: a Golgi study. Ann Neurol 1984; 16:595–602
41. Machado-Salas JP. Abnormal dendritic patterns and aberrant spine development of Bourneville's disease—a Golgi survey. Clin Neuropathol 1984;3:52–58
42. Kingsley DPE, Kendal BE, Fritz CT. Tuberous sclerosis: a clinico-radiological evaluation of 110 cases with reference of atypical presentation. Neuroradiology 1986;28:38–46
43. Boesel CP, Paulson GW, Kosnik EJ, Earle KM. Brain hamartomas and tumors associated with tuberous sclerosis. Neurosurgery 1979;4:410–417
44. Shepherd CW, Houser OW, Gomez MR. MR findings in tuberous sclerosis complex and correlation with seizure development and mental impairment. Am J Neuroradiol 1995;16:149–155
45. Curatolo P, Cusmai R, Pruna D. Tuberous sclerosis: diagnostic and prognostic problems. Pediatr Neurosci 1986;12:123–125
46. Roach ES, Williams DP, Laster DW. Magnetic resonance imaging in tuberous sclerosis. Arch Neurol 1987;44:301–304
47. Nixon JR, Houser OW, Gomez MR, Okazaki H. Cerebral tuberous sclerosis: MR imaging. Radiology 1989;170:869–873
48. Cusmai R, Chiron C, Curatolo P, et al. Topographic comparative study of magnetic resonance imaging and electroencephalography in 34 children with tuberous sclerosis. Epilepsia 1990; 31:747–755
49. Chugani HT, Rintahaka PJ, Shewmon DA. Ictal patterns of cerebral glucose utilization in children with epilepsy. Epilepsia 1994;35:813–822
50. Dailey JW, Reigel CE, Mishra PK, Jobe PC. Neurobiology of seizure predisposition in the genetically epilepsy-prone rat. Epilepsy Res 1989;3:317–320
51. Statnick MA, Dailey JW, Jobe PC, Browning RA. Abnormalities in brain serotonin concentration, high-affinity uptake, and tryptophan hydroxylase activity in severe-seizure genetically epilepsy-prone rats. Epilepsia 1996;37:311–321
52. Wenger GR, Stitzel RE, Craig CR. The role of biogenic amines in the reserpine-induced alteration of minimal electroshock seizure thresholds in the mouse. Neuropharmacology 1973;12: 693–703
53. Lazarova M, Bendotti C, Samanin R. Studies on the role of serotonin in different regions of the rat central nervous system on pentylenetetrazol-induced seizures and the effect of di-*n*-propyl-lacetate. Arch Pharmacol 1983;322:147–152
54. Pallister PD. Aggravation of epilepsy by reserpine, associated with possible bleeding and clotting disturbances. Rocky Mt Med J 1982;56:45–50
55. Maynert E, Marczynski T, Browning R. The role of neurotransmitters in the epilepsies. Adv Neurol 1975;13:79–147
56. Chugani DC, da Silva EA, Muzik O, et al. Abnormal serotonin synthesis in epileptic foci of children: an in vivo study with alpha[C-11]methyl-tryptophan and positron emission tomography. Twenty-second international epilepsy congress, Dublin, Ireland. Epilepsia 1997;38(Suppl 3):45 (Abstract)